https://doi.org/10.5194/egusphere-2026-3707
Preprint. Discussion started: 28 July 2026
© Author(s) 2026. CC BY 4.0 License.

Reviews and syntheses: Bridging Limnology and Satellite Methane Observations for Small Water Bodies

Anjali Wankhede[1], Yasser Morera-Gómez[2], Johannes Bühl[1], and Andrea Heilmann[1]
[1]Harz University of Applied Science, Wernigerode, 38855, Germany
[2]University of Navarra, BIOMA Institute for Biodiversity and the Environment, 31008, Pamplona, Spain

Correspondence: Anjali Wankhede (awankhede@hs-harz.de)

Abstract. Methane (CH_4) emissions from small freshwater bodies represent a significant yet poorly quantified component of the global greenhouse gas budget, even though lakes and ponds smaller than about 1 km^2 dominate the areal extent of inland standing waters worldwide and include the <50 ha size class considered here. The German Small Lake and Pond Inventory maps over 260,000 ponds and small lakes between 0.001 and 50 ha. This review focuses on ponds and small lakes in the approximate size range 0.001–50 ha, corresponding to the size classes that dominate the Germany's small lake and pond inventory and constitute a substantial share of the country's standing water surface area. Small lakes and ponds have been shown to emit methane at substantially higher areal rates than larger systems, but monitoring remains dominated by labor intensive in situ campaigns with limited spatial coverage. This systematic literature review synthesizes 30 peer reviewed publications from limnology, biogeochemistry, and Earth observation to assess whether current satellite remote sensing technologies can meaningfully contribute to quantifying methane emissions from small water bodies. The reviewed evidence reveals a fundamental scale and sensitivity mismatch typical small water bodies emit 0.01–1 kg CH_4 per hour, whereas satellite point source detection thresholds remain above 50 kg per hour, so their signals are below the instrument's detection limits. Moreover, each satellite pixel covers a large area, so the methane from one small pond is diluted inside a large pixel and cannot be separated from the surrounding landscape. Satellite algorithms including optimal estimation, proxy methods, and matched filters work well for global climate monitoring and detection. They have been successfully applied to global background monitoring and industrial super emitters have been successfully applied to global background monitoring and industrial super-emitters, but they have not been validated for inland waters at pond scale. Across the reviewed studies, the most promising approaches combine satellite derived optical proxies (e.g., chlorophyll, vegetation and temperature) with statistical or machine learning upscaling and atmospheric inversion, rather than direct satellite detection of individual ponds. Overall, this review concludes that current satellites cannot yet provide direct, observation based emission estimates for single small water bodies and identifies specific data integration and modeling pathways that future research should pursue to reduce this monitoring gap.

Keywords: methane emissions, small ponds, satellite remote sensing, TROPOMI, ebullition, methanogenesis, retrieval algorithms, systematic review

https://doi.org/10.5194/egusphere-2026-3707
Preprint. Discussion started: 28 July 2026
© Author(s) 2026. CC BY 4.0 License.

1 Introduction

1.1 The methane paradox

Methane (CH_4) is a key greenhouse gas in the climate system. Over a 20 year time horizon, its global warming potential is about 84 times that of carbon dioxide, while its atmospheric lifetime is only around 12 years, compared with decades to centuries for CO_2, making methane reductions particularly effective for near term climate mitigation (IPCC, 2023). The 26th Conference of Parties (COP26) Global Methane Pledge, calling for 30% emission reductions by 2030, reflects growing recognition that methane mitigation could slow warming more rapidly than CO reductions alone (Jiang et al., 2024).

Political discussions mainly emphasize anthropogenic methane sources such as oil and gas infrastructure, coal mines, livestock, but natural emissions from planet's numerous small water bodies receive far less attention. Freshwater inland lakes contribute an estimated 8–103 Tg CH_4 annually, approaching 20% of global natural emissions and potentially offsetting one-quarter of the terrestrial carbon sink on a CO equivalent basis (Bastviken et al., 2004; West et al., 2016). A central paradox is that the smallest lakes and ponds exhibit the highest methane emission rates per unit of area, yet they are also the water bodies least frequently monitored and quantified (Bastviken et al., 2004; West et al., 2016). In the dataset used in Wachholz et al. (2026) study, 89.9% of water bodies cover less than 1 ha, and 98.7% fall below 10 ha which is precisely the size range that lies below the detection threshold of every current satellite sensor (refer Figure 1).

1.2 Small water bodies are disproportionate emitters

The foundational understanding that small water bodies contribute disproportionately to atmospheric methane rests on Bastviken et al. (2004) global synthesis. Analyzing 85 lakes spanning five orders of magnitude in surface area, they documented an inverse relationship between lake size and methane flux per unit area (areal emission rates), with lake size explaining variance in emissions ($R^2 = 0.47$) and this relationship being statistically highly significant ($p < 0.001$), with the steepest gradient occurring below 100 hectares (ha) (Tranvik et al., 2009). This counterintuitive pattern reflects fundamental biogeochemical differences: shallow depths, high productivity, and limited oxidation capacity combine to create methane emission hotspots in the planet's smallest aquatic systems (Bastviken et al., 2004).

West et al. (2016) advanced this understanding with a study of 16 north-temperate lakes (0.2–69.7 ha), in which they measured both sediment methanogenesis and atmospheric methane fluxes. Lake productivity which is represented by chlorophyll-a concentration was positively related to methanogenesis rates ($R^2 = 0.32$, $p = 0.02$). However, this did not lead directly to higher diffusive emissions at the lake surface. The pathway of the produced methane depended strongly on water depth especially in lakes shallower than 6 m, a large fraction escaped as ebullition, that is, bubbles rising directly from the sediments to the atmosphere, whereas in deeper lakes 97.9–99.9% of methane was oxidized before reaching the surface(West et al., 2016).

In this study, "ponds" and "small lakes" are defined following the recent German Small Lake and Pond Inventory (GSLPI), which systematically mapped standing water bodies across Germany in the size range of 0.001-50 hectares (10–500,000 m^2) (Wachholz et al., 2026). Ponds are considered water bodies smaller than 5 ha (50,000 m^2), while small lakes are defined as 5-50 ha (50,000–500,000 m^2) (Wachholz et al., 2026).These thresholds were chosen because water bodies in this size range

https://doi.org/10.5194/egusphere-2026-3707
Preprint. Discussion started: 28 July 2026
© Author(s) 2026. CC BY 4.0 License.

are extremely numerous and dominate the standing water count in Germany, so that collectively they represent a substantial fraction of the national inland water surface and are expected to contribute disproportionately to methane emissions. Focusing on ponds and small lakes therefore targets the part of the size spectrum that is both abundant and currently under represented in large scale remote sensing and inventory products (Wachholz et al., 2026).

Figure 1 illustrates the size distribution of all 261,567 lakes and ponds in the GSLPI falling within the 0.001–50 ha range, out of 262,443 total mapped water bodies. The 0.1–1 ha class is by far the most populous, containing 150,908 water bodies that is 57.7% of the entire inventory. The 0.01–0.1 ha class is the second largest with 83,281 lakes (31.8%). Together, these two classes account for 89.5% of all mapped water bodies. The largest size classes are comparatively rare: the 1–10 ha class contains 22,881 lakes (8.7%) and the 10–50 ha class only 3,454 (1.3%). The smallest class, 0.001–0.01 ha, contains just 1,043 water bodies (0.4%), reflecting both genuine scarcity and the detection limits of the inventory. The cumulative distribution confirms that nearly 90% of all lakes are smaller than 1 ha and 98.7% are smaller than 10 ha. This size structure directly supports the rationale of this review that the German water landscape is numerically dominated by very small water bodies, and it is precisely these systems that current satellite sensors struggle to resolve. The lake area histogram (Fig. 1) was produced from the full German Small Lake and Pond Inventory dataset (Wachholz et al., 2026). Lake area values, originally recorded in square meters (m^2) in the inventory GeoPackage file, were converted to hectares (ha) and assigned to five log-scale size classes: 0.001–0.01, 0.01–0.1, 0.1–1, 1–10, and 10–50 ha. The bar chart displays the absolute count per class, and the overlaid line shows the cumulative percentage of lakes up to each class boundary. The figure was generated using Python (fiona, pandas, matplotlib).

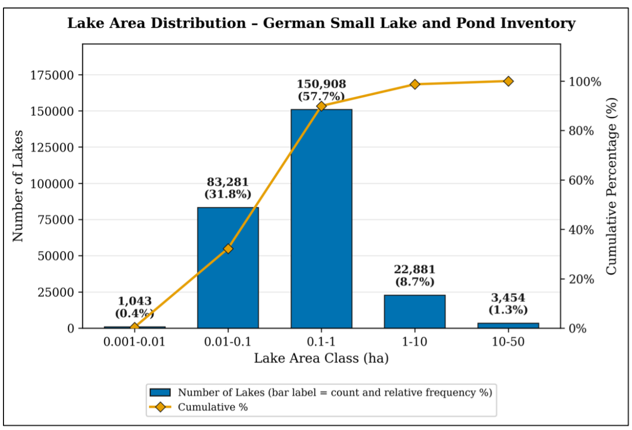

Figure 1. Size distribution of lakes and ponds in the Germany's Small Lake and Pond Inventory (n = 261,567; size range 0.001–50 ha). Bar chart: number of lakes per area class (ha). Line: cumulative percentage of lakes by area class. Data source: (Wachholz et al., 2026);dataset: (Wachholz, 2024).

https://doi.org/10.5194/egusphere-2026-3707
Preprint. Discussion started: 28 July 2026
© Author(s) 2026. CC BY 4.0 License.

1.3 The satellite remote sensing revolution

Parallel to advances in aquatic biogeochemistry, satellite remote sensing has transformed atmospheric methane monitoring. The lineage begins with SCIAMACHY aboard Envisat (2003–2009), the first satellite detecting near-surface methane via short-wave infrared (SWIR) absorption bands (Buchwitz et al., 2006). Japan's GOSAT, launched 2009 with its TANSO-FTS instrument, provided the first dedicated greenhouse gas observations, achieving 0.7% precision for column-averaged dry-air mixing ratios (XCH_4) at 10 km resolution((Butz et al., 2011; Parker et al., 2020).

The 2017 launch of TROPOMI aboard Sentinel-5 Precursor marked a watershed offering 5.5 × 7 km resolution, daily global coverage, and 0.8% precision (Hu et al., 2018; Veefkind et al., 2012). TROPOMI enables both climate-scale monitoring and detection of strong point sources (Lorente et al., 2021) . Lorente et al. (2021) found that TROPOMI XCH_4 agrees with ground based TCCON (Total Carbon Column Observing Network) measurements to within 1% across all stations, with an average bias of -0.2%. Looking ahead, MERLIN (Methane Remote Sensing Lidar Mission) a Franco-German satellite planned for launch in 2029 will use an active integrated path differential absorption (IPDA) lidar to measure atmospheric methane independently of solar illumination, extending coverage to polar regions and night-time conditions currently inaccessible to passive sensors (Ehret et al., 2017).

1.4 Research gap and objectives

This review confronts a question missing from published literature: Can satellite remote sensing technologies, developed for either global climate monitoring or industrial leak detection, detect and quantify methane emissions from small natural water bodies? This question is important for both science and policy. If satellites can reliably monitor methane emissions from small ponds, they would offer a practical way to reduce current gaps in methane budgets, assess the effects of eutrophication, and test process based models. If this is not feasible because of fundamental limits in sensor sensitivity or spatial resolution, then it is essential to recognize these limits and focus efforts on alternative monitoring approaches. This systematic review pursues three research questions:

1. RQ1: What biogeochemical processes drive methane emissions from small water bodies, how large are these emissions, and how do variables like water temperature, thermal stratification, wind speed, and solar radiation cause small systems to behave differently from large lakes?

2. RQ2: What satellite remote sensing technologies are available for methane detection, and to what extent do their current technical specifications actually allow detection and quantification of emissions from individual small water bodies?

3. RQ3: How can satellite derived proxies like water surface temperature, solar radiation, and wind fields be combined with in situ eddy covariance CH_4 flux measurements and modelling approaches to improve methane emission monitoring of small water bodies?

https://doi.org/10.5194/egusphere-2026-3707
Preprint. Discussion started: 28 July 2026
© Author(s) 2026. CC BY 4.0 License.

2 Methodology

This review followed established systematic review principles, adapted from quality assessment frameworks for systematic literature reviews (Alchokr et al., 2026; Kitchenham et al., 2009; Okoli and Schabram, 2010). We compiled and analysed literature between March and December 2025 and carried out the main database searches during October to December 2025.

2.1 Literature search strategy

A targeted search strategy across multiple databases was performed. A set of key foundational papers was first identified directly from the research questions, after which targeted searches were run across Web of Science, Scopus, and Google Scholar. These database results were then broadened through forward and backward citation tracking from the foundational papers to ensure no closely related work was missed. Three thematic search concepts guided our literature compilation, with a fourth concept added specifically to capture optical proxy retrieval studies relevant to indirect satellite-based emission estimation:

1. Methane Emissions: “methane emission*” OR “CH_4 flux*” OR “methanogenesis” OR “ebullition”
2. Aquatic Systems: “lake*” OR “pond*” OR “reservoir*” OR “freshwater” OR “inland water*”
3. Remote Sensing: “satellite” OR “remote sensing” OR “TROPOMI” OR “GOSAT” OR “Sentinel” OR “hyperspectral”
4. Optical Proxies: “chlorophyll*” OR “chlorophyll-a” OR “turbidity” OR “optical proxy” OR “water quality retrieval”

An asterisk (*) denotes a wildcard character, allowing for different word endings (for example, “flux” returns “flux” and “fluxes”). Records were screened against predefined inclusion and exclusion criteria (Table 1), covering publication type, time period, study environment, and thematic focus."

2.2 Data extraction and analysis

The relatively small number of papers ultimately included in this review are 30 out of 200 initially identified records which reflects the genuine scarcity of literature at the specific intersection of satellite remote sensing and methane emissions from small freshwater bodies. Of the 200 records identified, 105 were removed at the title and abstract screening stage, primarily because they dealt with large lakes, open oceans, estuarine systems, or wetlands without any pond component, or because they addressed greenhouse gas fluxes in a purely terrestrial context. This left 95 records for full-text assessment, of which a further 51 were excluded. The most common reasons were that studies used only ground-based or airborne measurement approaches with no satellite component, presented purely theoretical or modelling frameworks without empirical validation, or focused on CO rather than CH_4 as the primary flux of interest. A smaller subset was excluded because their spatial resolution or sensor specifications were reported at scales far too coarse to be relevant to sub-50 ha water bodies. Of the remaining 44 records, a final 14 were excluded after quality assessment, studies that lacked sufficient methodological transparency and did not report empirical validation of their approaches or presented findings that could not be independently verified from the reported data. The 30 papers that passed all criteria therefore reflect not a limitation of the search strategy, but the emerging and still narrow

https://doi.org/10.5194/egusphere-2026-3707
Preprint. Discussion started: 28 July 2026
© Author(s) 2026. CC BY 4.0 License.

Table 1. Inclusion and exclusion criteria applied during study selection.

Criterion	Included	Excluded
Publication type	Peer-reviewed journal articles; systematic review papers (for methodology only)	Non-peer-reviewed materials (except sample systematic review papers for methodology)
Time period	1993–2024 for core reviewed studies. Supporting references for inventory data, methodological frameworks, and satellite specifications are not subject to this restriction	Publications before 1993 or after 2024
Language	English	Non-English publications
Study environment	Freshwater systems like lakes, ponds, reservoirs	Marine or estuarine environments without a clear freshwater focus
Wetland scope	Wetland studies that include pond components	Wetland-only studies with no pond component
Thematic focus	Methane emissions from freshwater; satellite remote sensing methodology and algorithms; foundational biogeochemistry of emission mechanisms	Studies outside methane or freshwater remote sensing scope
Empirical basis	Studies combining modelling or theory with empirical measurements	Purely theoretical or modelling work with no empirical validation

nature of this research satellite-based observation of methane from individual small ponds and lakes remains an active but nascent field with a thin literature base. Several studies addressing optical proxy retrieval relevant to methane monitoring (e.g., (Giardino et al., 2015; Hestir et al., 2015; Tyler et al., 2016) were identified through forward and backward citation tracking from foundational papers rather than direct database search, reflecting the cross-disciplinary nature of optical proxy literature.

For each paper, we extracted:

- Bibliographic data: Authors, year, journal
- Study type: Empirical measurement, satellite methodology, synthesis/review
- Domain: Limnology, remote sensing, biogeochemistry, methodology
- Key findings: Emission magnitudes, satellite capabilities, algorithm performance
- Methodological details: Measurement approaches, sample sizes, validation procedures
- Relevance to RQs: The research questions the paper addresses.

The overall study-selection process is summarized in Fig. 2, from 200 initial records to 30 included peer-reviewed studies. We assessed included studies using adapted criteria from Alchokr et al. (2026) to ensure methodological quality. Quality scores

https://doi.org/10.5194/egusphere-2026-3707
Preprint. Discussion started: 28 July 2026
© Author(s) 2026. CC BY 4.0 License.

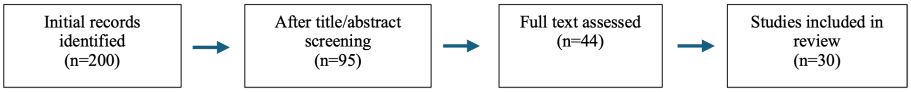

Figure 2. Simplified study-selection flow for the systematic literature review on satellite remote sensing of methane emissions from small water bodies.

were assigned based on clarity of research goals, justification of design decisions, thoroughness of methodology description, completeness of results reporting, evidence supporting findings, and feasibility of methods employed. For each remote sensing study, methane retrieval approaches were coded into three algorithm categories: physics-based spectral retrievals, data-driven matched-filter methods, and optical proxy models. This categorization was based on how the authors formulated the radiative transfer problem, the type of input data (spectral radiances vs. surface reflectance), and whether methane was retrieved directly or inferred from correlated optical indicators. These codes were later summarized in to support answering RQ2 on satellite technologies.

3 Results

3.1 Literature corpus overview

The 30 core papers span 1993–2024. Three additional references cited in this review which are Wachholz et al. (2026); Alchokr et al. (2026); Hancock et al. (2025) fall outside this range but serve as supporting references for inventory data, quality assessment methodology, and satellite specifications respectively, rather than as part of the systematic corpus. With publication activity increasing markedly after 2011 particularly studies focusing on satellite-based methane observation (GOSAT, TROPOMI). The 30 studies included in this review has publication dates ranging from 1993 to 2024, with a clear concentration in the more recent half of that range. Only a small number of studies were published before 2010. Publication frequency increased noticeably after 2017, coinciding with the launch of TROPOMI aboard Sentinel-5P, which substantially expanded the volume and precision of available satellite methane data. This pattern suggests that growth in this research area has tracked closely with advances in satellite instrumentation rather than following a steady or unrelated trend.

Fig. 3 shows the disciplinary composition of the corpus across the same timeline. Limnology and biogeochemistry dominate across all periods, while remote-sensing papers become more frequent in the GOSAT/TROPOMI era and dedicated methodological contributions remain rare. This pattern confirms that most evidence on small-water-body methane still comes from lake studies, with satellite methods only recently entering the field.

https://doi.org/10.5194/egusphere-2026-3707
Preprint. Discussion started: 28 July 2026
© Author(s) 2026. CC BY 4.0 License.

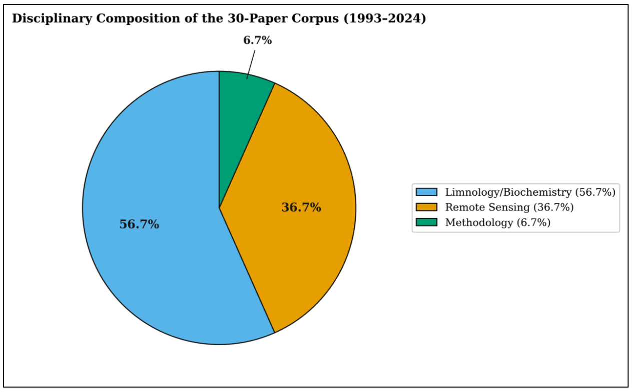

Figure 3. Disciplinary composition of the 30-paper corpus (1993-2024)

3.2 Methane emission mechanisms in small water bodies

3.2.1 The methanogenesis-ebullition coupling

West et al. (2016) provide a clear description of how methane is produced and released in small lakes. They showed that lake productivity, measured by chlorophyll a concentrations in the surface (epilimnetic) water, predicts how much methane can be produced in the sediments (methanogenesis potential; $R^2 = 0.32$, $p = 0.02$). This happens because algae supply fresh, nitrogen rich organic matter that microbes can decompose easily, which speeds up methanogenesis compared with hard to degrade terrestrial material.

Despite this high production, surface water methane concentrations remained uniform (0.13–0.76 μM (micromolar)) even though bottom waters ranged from 0.26 to 1362.64 μM. In stratified summer conditions, 97.9–99.9% of the methane produced in sediments is either consumed by methane oxidizing bacteria near the sediment–water interface and the transition from oxygenated to oxygen poor water, or it stays trapped in the anoxic deep layer. Where emissions were high, they were dominated by ebullition. Bubble formation requires methane concentrations above saturation (around 1.5 mM at 25°C and standard sea level atmospheric pressure) and enough gas pressure to overcome the weight of the overlying water and the resistance of the sediments. West et al. (2016) found that bubble release is most likely when methanogenesis rates are high (supplying methane to porewaters) and when water depth is shallow (<6 m), which reduces hydrostatic pressure and allows bubbles to reach the surface. For the Hotspot Phenomena, DelSontro et al. (2011, 2016) established methane ebullition as an extraordinarily heterogeneous process. Analyzing northern lakes, they found ebullition concentrated in hotspots comprising 10–30% of lake area yet generating 50–80% of total emissions (DelSontro et al., 2011, 2016). Hotspot locations correlate with organic-rich sediments in shallow depositional zones. Environmental controls on methane emissions from small water bodies operate across three distinct tiers which are primary controls that directly drive methane production and bubble release, secondary controls that modulate the intensity of those processes, and tertiary landscape-level factors that set the broader context in which the primary controls operate (West et al., 2016; Bastviken et al., 2004; Deemer et al., 2016; Davidson et al., 2015)(Table 2).

https://doi.org/10.5194/egusphere-2026-3707
Preprint. Discussion started: 28 July 2026
© Author(s) 2026. CC BY 4.0 License.

Table 2. Environmental controls on CH_4 emissions from small water bodies.

Primary Controls	Secondary Controls	Tertiary Controls
Water Column Depth	Organic Matter Quality	Lake Size
Productivity / Trophic Status (chlorophyll-a)	Hydrostatic Pressure	Catchment Land Use
Temperature	Sediment Properties	Fetch / Exposure

The primary controls depth, productivity, and temperature are the variables most accessible to remote sensing, through bathymetric mapping, chlorophyll-a retrieval and land surface temperature products respectively, making them the logical foundation for any satellite-based emission proxy (Duan et al., 2023; Giardino et al., 2015; West et al., 2016). Second, because tertiary landscape factors operate through the primary controls rather than independently, catchment variables such as land use can be incorporated into regional emission models without requiring direct measurement of every intermediate process (Davidson et al., 2015; Webb et al., 2019).

3.2.2 Quantitative summary of emission magnitudes

Emission magnitudes from different lakes were reported by West et al. (2016). Satellite point source algorithms report methane plumes as “total emission rates” (kg CH_4 hr^{-1}[a]), the mass released per hour from a source. To compare, we convert West et al. (2016) areal fluxes to kg hr^{1} for a typical 0.5 ha pond using the following steps.

Step 1 – Total molar emission per day:

$$n = F \times A \tag{1}$$

where F is the areal flux $(\mathrm{mmol\,CH_4\,m^{-2}\,d^{-1}})$ and A is the pond area $(\mathrm{m^2})$. For a 0.5 ha pond ($A = 5000\,\mathrm{m^2}$) with $F = 4.709\,\mathrm{mmol\,m^{-2}\,d^{-1}}$:

$$n = 4.709 \times 5000 = 23{,}545\,\mathrm{mmol\,d^{-1}} \tag{2}$$

Step 2 – Convert moles to mass per day:

$$m_{\mathrm{day}} = n \times M_{\mathrm{CH_4}} \tag{3}$$

where $M_{\mathrm{CH_4}} = 16\,\mathrm{g\,mol^{-1}}$:

$$m_{\mathrm{day}} = 23{,}545 \times 16 = 376.72\,\mathrm{g\,d^{-1}} \tag{4}$$

[a] kg hr^{-1} = kilograms of methane per hour; universal for industrial sources (50–5000 kg hr^{-1}), ponds (0.01–0.5 kg hr^{-1}). mmol m^{-2} d^{-1} = millimoles per square meter per day (areal flux). X_{CH_4} (ppb) = atmospheric column enhancement.

https://doi.org/10.5194/egusphere-2026-3707
Preprint. Discussion started: 28 July 2026
© Author(s) 2026. CC BY 4.0 License.

Step 3 – Convert to $\mathrm{kg\,h^{-1}}$:

$$m_{\text{hour}} = \frac{m_{\text{day}}}{24 \times 1000} = \frac{376.72}{24{,}000} \approx 0.0157\,\mathrm{kg\,h^{-1}} \tag{5}$$

Applying this formula across the three study lakes gives:

Table 3. Converted methane emission rates for three lakes (West et al., 2016) scaled to a 0.5 ha pond.

Lake	Areal flux ($\mathrm{mmol\,m^{-2}\,d^{-1}}$)	Total emission ($\mathrm{kg\,h^{-1}}$)	Emission class
Paul Lake	4.709	0.0157	High
Morris Lake	3.302	0.0110	Moderate
Crampton Lake	0.026	0.0000867	Low

These emission rates are roughly 10^3–10 times lower than current satellite point source detection limits (see RQ 2). The three lakes span the productive range documented by West et al. (2016): Paul Lake is the most productive (highest chlorophyll-a), Morris Lake is intermediate, and Crampton Lake is oligotrophic with minimal methanogenesis. The emission class column reflects this gradient that the high, moderate and low correspond to eutrophic, mesotrophic, and oligotrophic conditions respectively and represents the realistic range a small pond in a temperate agricultural landscape would occupy depending on its nutrient status. The significance of these emission magnitudes in relation to satellite detection limits is assessed in Sect. 3.4.

3.3 Satellite remote sensing technologies

3.3.1 Satellite retrieval algorithms relevant to small water bodies

Remote sensing studies used three main retrieval approaches for methane over aquatic or semi-aquatic environments: physics-based spectral retrievals, data-driven matched filters, and optical proxy models. To illustrate their strengths and limitations for small water bodies, Table 4 summarises how these algorithm work, their key advantages and constraints, and representative applications in the literature.

Within the physics based category, two specific implementations are relevant to the historical satellite record WFM-DOAS and IMAP-DOAS, both developed for SCIAMACHY-based atmospheric methane monitoring (Buchwitz et al., 2006; Frankenberg et al., 2011). WFM-DOAS achieves this through a fast Taylor-series linearisation of the Lambert–Beer law, keeping processing times tractable across wide satellite swaths (Buchwitz et al., 2006), while IMAP-DOAS iterates toward a maximum a posteriori solution, gaining tighter posterior uncertainty at the cost of computational throughput (Frankenberg et al., 2011). Both algorithms were designed and validated against large, bright land surfaces with high and spectrally structured reflectance (Buchwitz et al., 2006). Over water the physics changes fundamentally like the dark, featureless surface suppresses the signal-to-noise ratio sharply, and a pond smaller than 50 ha contributes so little methane to the overlying column that its signal is indistinguishable from retrieval noise before any detection threshold is reached (Lorente et al., 2021). The expected signal therefore remains below the retrieval sensitivity required for reliable detection.

https://doi.org/10.5194/egusphere-2026-3707
Preprint. Discussion started: 28 July 2026
© Author(s) 2026. CC BY 4.0 License.

Table 4. Comparative analysis of satellite retrieval algorithms for methane detection in aquatic and semi-aquatic environments.

Feature	OEM (GOSAT)[a]	Remote Algorithm (TROPOMI)[b]	CO_2 Proxy Method[c]	Matched Filter[d]
Mathematical basis	Bayesian inverse radiative transfer	Phillips–Tikhonov regularisation	Column ratio: X_{CH_4}/X_{CO_2}	Data-driven spectral template matching
Output	CH_4 vertical profile + averaging kernels	Total column X_{CH_4}	X_{CH_4} proxy	Column enhancement (ppm·m)
Spatial resolution	∼10 km (coarse)	5.5 × 3.5 km	Sensor-dependent	Sub-pixel to ∼30 m (airborne)
Processing speed	Minutes per pixel	Daily global coverage	Near real-time	Sub-second per pixel
Uncertainty quantification	Rigorous (full posterior)	Moderate (regularised)	Limited; CO_2 model dependent	Low and no formal uncertainty
Aerosol sensitivity	Explicit retrieval	Simultaneous fit	Partially cancelled by proxy	Not corrected
Bias vs. TCCON	<1 % (well-characterised)	<0.6 %	Seasonal CO_2 gradient bias	High false positive rate
Detection scale	Regional/global background	Regional/global X_{CH_4}	Regional/global X_{CH_4}	Point sources (50–300 kg/h)
Best suited for	Scientific accuracy, profiling	Operational global monitoring	Computationally simple regional surveys	Industrial leak detection, super-emitters
Key limitation	Computationally intensive; needs accurate priors	No vertical information	CO_2 model uncertainty; seasonal bias	High false positives; requires validation

[a](Butz et al., 2011; Frankenberg et al., 2011). [b](Lorente et al., 2021; Veefkind et al., 2012). [c](Butz et al., 2011; Frankenberg et al., 2011). [d](Ayasse et al., 2019; Cusworth et al., 2019; Varon et al., 2018).

Matched-filter methods sidestep the radiative-transfer problem by asking a statistically simpler question which does this pixel look anomalous relative to its neighbors within the methane absorption bands? The filter projects each pixel's radiance onto a target methane spectrum and flags pixels whose spectral residual exceeds a detection threshold an approach that is fast, resolution-friendly, and well-suited to detecting sparse point-source plumes against spectrally uniform backgrounds. These properties explain why matched-filter algorithms have become the method of choice for next-generation imaging spectrometers such as EnMAP, PRISMA, and EMIT, where the target is typically an industrial facility emitting a compact, localized plume (Ayasse et al., 2019; Guanter et al., 2015; Jiang et al., 2024). Small water bodies violate both design assumptions simultaneously. The background is spectrally noisy because dark water produces low and variable reflectance that inflates the false-positive rate and the emission itself is diffuse, spread across an entire pond surface rather than concentrated into the tight spectral spike the filter is optimised to catch. Even integrating deep learning into the matched-filter pipeline, the lowest detec-

https://doi.org/10.5194/egusphere-2026-3707
Preprint. Discussion started: 28 July 2026
© Author(s) 2026. CC BY 4.0 License.

tion thresholds reported with EnMAP and PRISMA remain around 500 kg h^{-1} (Guanter et al., 2015; Jiang et al., 2024) several orders of magnitude above the <1 kg h^{-1} typical of a small eutrophic pond.

Optical proxy methods follow a different logic entirely, bypassing atmospheric retrieval and instead using the water surface itself as the measurement medium. Instruments such as Landsat 8 and Sentinel-2 provide surface reflectance bands sensitive to water turbidity and chlorophyll concentration, and where those optical properties co-vary with dissolved methane in the water column, the satellite image becomes an indirect proxy for emission potential (Morozumi et al., 2019). Morozumi et al. (2019) demonstrated this approach convincingly during Siberian flood events, using spectral contrasts to separate methane-rich tributaries from methane-poor main channels; more recent Sentinel-2 turbidity models have achieved R^2 values above 0.90 for inland water optical retrievals (Leggesse et al., 2024). The fundamental ceiling is that the turbidity-to-methane relationship is not transferable, it shifts with lake trophic state, season, sediment composition, and catchment land use, meaning every new site requires an independent field calibration campaign before the proxy can be applied with confidence.

3.3.2 Area flux mappers vs. Point source imagers

Following Jiang et al. (2024)satellite methane sensors divide into two categories, each designed for a distinct observational objective and carrying trade-offs that directly determine their suitability for small water bodies (Table 5).

Table 5. Characteristics of the two main satellite sensor categories used for methane detection.

Characteristic	Area flux mappers	Point source imagers
Primary purpose	Global or regional X_{CH_4} distribution for climate science	Individual emission plume detection for industrial monitoring
Spatial resolution	1–10 km	20–100 m
Temporal resolution	Daily to weekly	5–16 days
Precision / detection threshold	<1 % precision for climate trend detection	>50 kg h^{-1} emission rate
Representative sensors	GOSAT/TANSO-FTS, TROPOMI, GOSAT-2, planned MERLIN (Hancock et al., 2025; Jacob et al., 2016)	Sentinel-2/MSI, Landsat-8/OLI, PRISMA, GaoFen-5/AHSI

The two categories expose a structural gap that small water bodies fall into rather than bridging. Area flux mappers such as GOSAT and TROPOMI achieve sub-1% precision for detecting long-term concentration trends across large regions, but their kilometer-scale pixels average methane signals over entire landscapes. A 0.5 ha pond occupies just 0.013% of a single TROPOMI pixel, contributing a signal indistinguishable from retrieval noise (Lorente et al., 2021; Veefkind et al., 2012). Point-source imagers such as PRISMA and Sentinel-2 offer 20–30 m resolution sufficient to geometrically resolve a pond, but their detection algorithms are calibrated for concentrated industrial plumes at 50–300 kg CH_4 hr^{-1} that is three to four orders of

https://doi.org/10.5194/egusphere-2026-3707
Preprint. Discussion started: 28 July 2026
© Author(s) 2026. CC BY 4.0 License.

magnitude above the 0.01–0.016 kg hr^{-1} typical of a small eutrophic pond (Cusworth et al., 2018; Guanter et al., 2021; Varon et al., 2021). The quantitative implications of this two-sided gap are assessed in Sect. 3.4. Neither category was designed for diffuse, low-intensity natural emitters, and this is the central constraint this review identifies.

3.4 Satellite detection feasibility

Direct detection of methane from small water bodies faces a two-sided barrier: spatial resolution and emission magnitude. Area flux mappers cannot resolve individual ponds like TROPOMI's 5.5 × 7 km pixel (38.5 km^2) means a 0.5 ha pond (0.005 km^2) occupies just 0.013% of a single pixel, so even at maximum emission rate its contribution to pixel-integrated XCH_4 falls 10× below single-pixel noise level (Lorente et al., 2021; Veefkind et al., 2012). Point-source imagers such as Sentinel-2, Landsat-8, and PRISMA provide metre-scale resolution adequate to geometrically contain a small pond and have demonstrated the ability to detect strong methane plumes from industrial super-emitters (Duren et al., 2019; Guanter et al., 2021; Varon et al., 2021), even TROPOMI, despite its coarser kilometre-scale pixels, has occasionally detected the very largest oil and gas "ultra-emitters" (Lauvaux et al., 2022). However PRISMA's path-integrated detection limit of 100 ppm·m for favourable plumes still remains two to three orders of magnitude above typical pond emission rates (Ayasse et al., 2019; Guanter et al., 2021; Jongaramrungruang et al., 2019). The technical specifications underlying these constraints are summarised in Table 6.

Table 6. Technical specifications of major methane remote sensing satellites.

Satellite/Sensor	Launch	Spatial resolution	Revisit	Spectral bands	Precision	Application
Area Flux Mappers						
GOSAT/TANSO-FTS[a]	2009	10 × 10 km	3 days	1.65, 2.3 µm	0.7 %	Global climate
TROPOMI/S5P[b]	2017	5.5 × 7 km	Daily	2.3 µm	0.8 %	Regional; some point sources
GOSAT-2[c]	2018	9.7 × 9.7 km	6 days	1.65, 2.3 µm	0.26 %	Enhanced global
Point Source Imagers						
Sentinel-2/MSI[d]	2015/2017	20 m	5 days	1.61, 2.19 µm	–	Land surface
Landsat-8/OLI[d]	2013	30 m	16 days	1.56–2.29 µm	–	Land cover
PRISMA[e]	2019	30 m	7 days	1.0–2.5 µm	∼100 ppm·m	Hyperspectral

[a](Butz et al., 2011; Parker et al., 2020). [b](Hu et al., 2018; Jacob et al., 2016; Lorente et al., 2021; Veefkind et al., 2012). [c](Suto et al., 2021). [d](Cusworth et al., 2018; Varon et al., 2021). [e](Ayasse et al., 2019; Guanter et al., 2021).

3.4.1 Emission magnitude mismatch

Cusworth et al. (2018) and Varon et al. (2021) established matched-filter detection limits for point-source imagers: reliable detection requires >300 kg h^{-1}, marginal detection is possible at 100–300 kg h^{-1} (54% success rate), and the practical lower bound under ideal conditions is 50 kg h^{-1}. These thresholds were independently confirmed by a 2024 multi-satellite blind test, which found that even the most sensitive current systems cannot reliably detect plumes below 60–200 kg h^{-1} (Sherwin

https://doi.org/10.5194/egusphere-2026-3707
Preprint. Discussion started: 28 July 2026
© Author(s) 2026. CC BY 4.0 License.

et al., 2024). Small water body emissions from Sect. 3.2 fall far below this floor: high emitters reach 0.0157 kg h^{-1}, moderate emitters 0.0110 kg h^{-1}, and typical emitters 0.01–0.03 kg h^{-1} approximately 10^3–10^4 times below detection thresholds. Table 7 summarises the combined feasibility assessment across both sensor categories.

Table 7 assesses the feasibility of direct satellite-based methane detection from small freshwater bodies across two sensor categories. The fundamental barrier is two-fold which is spatial resolution and emission magnitude. Regarding spatial resolution, area flux mappers such as TROPOMI operate at pixel sizes of 5.5 × 7 km, which physically precludes the isolation of individual ponds which is a limitation consistent with findings that small water bodies below approximately 0.1 ha remain invisible to coarse-resolution sensors (Jacob et al., 2016; Veefkind et al., 2012). Point-source imagers such as PRISMA offer 30 m SWIR resolution, which is geometrically adequate for ponds exceeding 0.1 ha, yet their detection thresholds of 50–300 kg CH_4 hr^{-1} remain orders of magnitude above the emission rates documented from small freshwater systems (0.00009–0.0157 kg hr^{-1}, Sect. 3.2; Bastviken et al., 2004; Deemer et al., 2016). Independent validation of this detection floor is provided by a 2024 multi-satellite blind test, which confirmed that even the most sensitive current systems cannot reliably detect plumes below approximately 60–200 kg hr^{-1} (Sherwin et al., 2024). This aligns with evidence that methane emissions from small ponds are systematically underestimated in national inventories, precisely because current remote sensing tools lack the sensitivity to capture them (Bastviken et al., 2011; IPCC, 2023). The combined spatial and radiometric constraints confirm that direct detection of pond-scale methane using existing satellite infrastructure remains currently infeasible, and that progress depends on next-generation sensors with less than 10 kg/hr detection floors. This directly answers RQ2 that is current satellite technologies, regardless of category, cannot detect or quantify methane emissions from individual small water bodies.

Table 7. Satellite detection feasibility assessment for small water bodies.

Criterion	Area flux mappers	Point source imagers	Assessment
Spatial resolution	5.5 × 7 km	30 m SWIR	Area: cannot resolve individual ponds. Point: adequate for ponds >0.1 ha
Detection threshold	∼15 kg/pixel	∼50–300 kg/hour	Pond emissions ∼10^3–10^4× too low for both
Overall feasibility	Infeasible	Currently infeasible	Direct detection not viable with existing sensors

3.5 Alternative approaches and future directions

Given the detection constraints established in Sect. 3.4, attention shifts to indirect approaches that map pond characteristics correlated with emission potential rather than methane itself. Among optical proxies, chlorophyll-a has the strongest mechanistic basis. Satellite-derived chlorophyll-a tracks epilimnetic productivity, which predicts sediment methanogenesis potential West et al. (2016) and has been directly used as a predictive input for satellite-based methane emission estimation in a large

https://doi.org/10.5194/egusphere-2026-3707
Preprint. Discussion started: 28 July 2026
© Author(s) 2026. CC BY 4.0 License.

eutrophic lake using machine learning models (R^2 = 0.65) (Duan et al., 2023), though this validation comes from a lake far larger than the size range addressed in this review, and it remains untested whether the same relationship holds at the below 50 ha scale. Sentinel-2 and Landsat-8 retrieve it at 20–30 m resolution sufficient to resolve individual ponds larger than approximately 0.1 ha. Recent inland water optical models have achieved R^2 values above 0.90 for chlorophyll-a and turbidity retrievals over inland waters (Leggesse et al., 2024). The constraint is transferability: the chlorophyll-a to methane relationship requires site-specific calibration because it shifts with season, trophic state, and catchment land use (Giardino et al., 2015). Beyond chlorophyll-a, hyperspectral sensors such as PRISMA and EnMAP enable simultaneous retrieval of suspended particulate matter and submerged aquatic vegetation, which together map the organic substrate supply driving methanogenesis (Guanter et al., 2015; Giardino et al., 2015; Hestir et al., 2015; Tyler et al., 2016).

Atmospheric inversion offers a complementary approach at regional scale. Combining TROPOMI XCH_4 observations with prior emission estimates from inventories or process models, inversion frameworks constrain total methane flux from pond-rich landscapes while propagating uncertainty from both data sources (Jacob et al., 2016; Maasakkers et al., 2022). The limitation is that inversion operates at grid scales of kilometers and cannot attribute emissions to individual ponds or size classes, but it can test whether regional inventory-based estimates are consistent with atmospheric observations.

Looking ahead, next-generation hyperspectral missions with improved signal-to-noise ratios could lower matched-filter detection thresholds below the current 500 kg h^{-1} floor, though closing the full 10^3–10^4 gap to pond-scale emissions is not achievable with near-term sensor architectures. The more immediately feasible direction is machine-learning upscaling that combines satellite-derived optical proxies like chlorophyll-a, surface temperature, turbidity with eddy covariance flux measurements from representative ponds to produce spatially continuous emission estimates without requiring direct methane detection (Deemer et al., 2016; West et al., 2016).

4 Discussion

Satellite observations of atmospheric methane have become remarkably powerful over the last two decades, delivering routine global maps of column-averaged concentrations and revealing major anthropogenic hotspots. Yet as this review makes clear, small lakes and ponds remain largely invisible to satellite-based assessments a consequence of sensors designed for different targets altogether. Current satellites were built either for kilometre-scale climate monitoring or for detecting concentrated industrial plumes, and small water bodies fit neither category.

This has a direct implication for what this review could and could not find. The inclusion criteria restricting to satellite remote sensing of methane from freshwater systems with empirical validation were necessary to keep the review focused, but they also excluded methodological literature from marine and wetland remote sensing that has developed proxy retrieval approaches potentially transferable to small ponds. Relaxing the freshwater constraint would likely surface additional chlorophyll-a and turbidity retrieval methods validated over optically complex waters, directly relevant to the proxy approaches identified in Sect. 3.5. This represents a limitation of the current review and a direction for future synthesis work.

https://doi.org/10.5194/egusphere-2026-3707
Preprint. Discussion started: 28 July 2026
© Author(s) 2026. CC BY 4.0 License.

Among the proxy approaches reviewed, chlorophyll-a retrieval stands out as both the most mechanistically justified and the most practically constrained. West et al. (2016) provide a direct empirical link between epilimnetic chlorophyll-a and sediment methanogenesis, but the chlorophyll-a to methane relationship is not universal. It varies with organic matter quality (West et al., 2012), trophic state (Davidson et al., 2015), and the balance between diffusive and ebullitive pathways (DelSontro et al., 2016), meaning a satellite-derived chlorophyll-a map cannot be converted to a methane flux map without site-specific calibration. Atmospheric inversion sidesteps this by operating at regional scales where individual pond variability averages out but loses the ability to attribute emissions to specific water bodies or size classes precisely the information needed to evaluate pond contributions within the GSLPI. Neither approach alone is sufficient; a robust monitoring strategy requires both, optical proxies for spatial pattern and inversion for regional flux constraint.

A further limitation concerns ebullition. All proxy approaches reviewed map variables linked to diffusive methane flux, chlorophyll-a, productivity, temperature but ebullition, which dominates emissions from the shallowest and most productive ponds (DelSontro et al., 2011; West et al., 2016), is spatially heterogeneous at scales of meters and episodic in timing. No current satellite proxy captures this pathway reliably. Until eddy covariance or acoustic bubble detection datasets are large enough to characterize ebullition patterns across the GSLPI size range, satellite-based upscaling will systematically underestimate total emissions from the smallest and most active ponds.

5 Conclusion

This review assessed whether current satellite remote sensing technologies can detect and quantify methane emissions from small water bodies in the size range covered by the German Small Lake and Pond Inventory. The reviewed literature shows that current systems cannot. Typical pond emissions of 0.01–0.016 kg CH_4 hr^{1} fall 10^{3}–10 times below the practical detection floor of the most sensitive point-source imaging systems, and area flux mappers operate at pixel scales that dwarf the ponds themselves.

The review also identifies secondary finding with practical implications. Satellites cannot detect methane from individual ponds, but they can map lake productivity specifically chlorophyll-a concentration at spatial resolutions approaching pond scale. Since chlorophyll-a is empirically linked to sediment methanogenesis, satellite-derived productivity maps represent a realistic near-term pathway to emission estimation rather than direct detection. Combined with atmospheric inversion at regional scales and eddy covariance validation at representative sites, this hybrid approach could produce the first spatially continuous methane emission estimates for pond-rich landscapes such as those catalogued in the GSLPI.

One approach that does not require next-generation sensors is to combine in situ flux measurements from larger, satellite-resolvable water bodies with optical proxy retrievals, then scale the derived emission relationships down to smaller ponds using inventory size distributions such as the GSLPI. Progress beyond this will depend on next-generation sensors with detection thresholds below 10 kg hr^{1} and systematic field campaigns that calibrate chlorophyll-a to methane relationships across the trophic gradient of small water bodies. Until both are in place, the methane flux from small freshwater systems will remain under quantified and therefore absent from current satellite-based greenhouse gas budgets.

https://doi.org/10.5194/egusphere-2026-3707
Preprint. Discussion started: 28 July 2026
© Author(s) 2026. CC BY 4.0 License.

Data availability. The lake and pond size distribution shown in Fig. 1 was derived from the German Small Lake and Pond Inventory (GSLPI) dataset (Wachholz, 2024),openly accessible via Zenodo at https://doi.org/10.5281/zenodo.14228168. No other primary datasets were generated or analysed during this study. All reviewed literature is cited in the reference list.

Author contributions. Dr. Andrea Heilmann and Anjali Wankhede identified the research gap and contributed to the conceptual framing of the study. Anjali Wankhede wrote the original draft and performed the manuscript revision. Dr. Yasser Morera Gomez contributed to the lake proxy and related sections and provided suggestions for improving the manuscript. Dr. Johannes Buehl contributed to the satellite data-related sections and provided suggestions for improving the manuscript. Dr. Andrea Heilmann also provided substantial editorial input. All authors contributed suggestions during manuscript development, and Anjali Wankhede incorporated the revisions and prepared the final version. All authors reviewed and approved the submitted manuscript.

Competing interests. The authors declare that they have no conflict of interest.

Acknowledgements. This research is supported by Project InterGrad. The authors gratefully acknowledge Prof. Dr. Andrea Heilmann, Dr. Yasser Gomez, and Prof. Dr. Johannes Buehl for their invaluable guidance and support throughout the completion of this work. During the preparation of this manuscript, the author used Claude (Claude Sonnet 4.6, Anthropic) for language editing, grammar and consistency checking, and proofreading of the draft text. The scientific content, data analysis, interpretation of results, and conclusions are entirely the work of the authors. The authors take full responsibility for the content of this publication.

Financial support.

This publication was funded by European Social Fund (ESF+) and the state of Saxony-Anhalt, as part of the InterGrad-EGD project [funding reference: ZS/2023/11/181808].

https://doi.org/10.5194/egusphere-2026-3707
Preprint. Discussion started: 28 July 2026
© Author(s) 2026. CC BY 4.0 License.

References

Alchokr, R., Sunilkumar, A., Saake, G., Leich, T., and Krüger, J.: A Comparative Analysis of Support Techniques for Assessing the Quality of Systematic Literature Reviews, in: Linking Theory and Practice of Digital Libraries, vol. 16097, edited by: Balke, W.-T., Golub, K., Manolopoulos, Y., Stefanidis, K., and Zhang, Z., Springer Nature Switzerland, Cham, 395–411, https://doi.org/10.1007/978-3-032-05409-8_23, 2026.

Ayasse, A. K., Dennison, P. E., Foote, M., Thorpe, A. K., Joshi, S., Green, R. O., Duren, R. M., Thompson, D. R., and Roberts, D. A.: Methane Mapping with Future Satellite Imaging Spectrometers, Remote Sens., 11, 3054, https://doi.org/10.3390/rs11243054, 2019.

Bastviken, D., Cole, J., Pace, M., and Tranvik, L.: Methane emissions from lakes: Dependence of lake characteristics, two regional assessments, and a global estimate, Glob. Biogeochem. Cycles, 18, 2004GB002238, https://doi.org/10.1029/2004GB002238, 2004.

Bastviken, D., Tranvik, L. J., Downing, J. A., Crill, P. M., and Enrich-Prast, A.: Freshwater Methane Emissions Offset the Continental Carbon Sink, Science, 331, 50–50, https://doi.org/10.1126/science.1196808, 2011.

Buchwitz, M., De Beek, R., Noël, S., Burrows, J. P., Bovensmann, H., Schneising, O., Khlystova, I., Bruns, M., Bremer, H., Bergamaschi, P., Körner, S., and Heimann, M.: Atmospheric carbon gases retrieved from SCIAMACHY by WFM-DOAS: version 0.5 CO and CH_4 and impact of calibration improvements on CO2 retrieval, Atmospheric Chem. Phys., 6, 2727–2751, https://doi.org/10.5194/acp-6-2727-2006, 2006.

Butz, A., Guerlet, S., Hasekamp, O., Schepers, D., Galli, A., Aben, I., Frankenberg, C., Hartmann, J.-M., Tran, H., Kuze, A., Keppel-Aleks, G., Toon, G., Wunch, D., Wennberg, P., Deutscher, N., Griffith, D., Macatangay, R., Messerschmidt, J., Notholt, J., and Warneke, T.: Toward accurate CO2 and CH_4 observations from GOSAT: GOSAT CO2 AND CH_4 VALIDATION, Geophys. Res. Lett., 38, n/a–n/a, https://doi.org/10.1029/2011GL047888, 2011.

Cusworth, D. H., Jacob, D. J., Sheng, J.-X., Benmergui, J., Turner, A. J., Brandman, J., White, L., and Randles, C. A.: Detecting high-emitting methane sources in oil/gas fields using satellite observations, Atmospheric Chem. Phys., 18, 16885–16896, https://doi.org/10.5194/acp-18-16885-2018, 2018.

Cusworth, D. H., Jacob, D. J., Varon, D. J., Chan Miller, C., Liu, X., Chance, K., Thorpe, A. K., Duren, R. M., Miller, C. E., Thompson, D. R., Frankenberg, C., Guanter, L., and Randles, C. A.: Potential of next-generation imaging spectrometers to detect and quantify methane point sources from space, Atmospheric Meas. Tech., 12, 5655–5668, https://doi.org/10.5194/amt-12-5655-2019, 2019.

Davidson, T. A., Audet, J., Svenning, J.-C., Lauridsen, T. L., Søndergaard, M., Landkildehus, F., Larsen, S. E., and Jeppesen, E.: Eutrophication effects on greenhouse gas fluxes from shallow-lake mesocosms override those of climate warming, Glob. Change Biol., 21, 4449–4463, https://doi.org/10.1111/gcb.13062, 2015.

Deemer, B. R., Harrison, J. A., Li, S., Beaulieu, J. J., DelSontro, T., Barros, N., Bezerra-Neto, J. F., Powers, S. M., dos Santos, M. A., and Vonk, J. A.: Greenhouse Gas Emissions from Reservoir Water Surfaces: A New Global Synthesis, BioScience, 66, 949–964, https://doi.org/10.1093/biosci/biw117, 2016.

DelSontro, T., Kunz, M. J., Kempter, T., Wüest, A., Wehrli, B., and Senn, D. B.: Spatial Heterogeneity of Methane Ebullition in a Large Tropical Reservoir, Environ. Sci. Technol., 45, 9866–9873, https://doi.org/10.1021/es2005545, 2011.

DelSontro, T., Boutet, L., St-Pierre, A., Del Giorgio, P. A., and Prairie, Y. T.: Methane ebullition and diffusion from northern ponds and lakes regulated by the interaction between temperature and system productivity, Limnol. Oceanogr., 61, https://doi.org/10.1002/lno.10335, 2016.

Duan, H., Xiao, Q., Qi, T., Hu, C., Zhang, M., Shen, M., Hu, Z., Wang, W., Xiao, W., Qiu, Y., Luo, J., and Lee, X.: Quantification of Diffusive Methane Emissions from a Large Eutrophic Lake with Satellite Imagery, Environ. Sci. Technol., 57, 13520–13529, https://doi.org/10.1021/acs.est.3c05631, 2023.

Duren, R. M., Thorpe, A. K., Foster, K. T., Rafiq, T., Hopkins, F. M., Yadav, V., Bue, B. D., Thompson, D. R., Conley, S., Colombi, N. K., Frankenberg, C., McCubbin, I. B., Eastwood, M. L., Falk, M., Herner, J. D., Croes, B. E., Green, R. O., and Miller, C. E.: California's methane super-emitters, Nature, 575, 180–184, https://doi.org/10.1038/s41586-019-1720-3, 2019.

Ehret, G., Bousquet, P., Pierangelo, C., Alpers, M., Millet, B., Abshire, J., Bovensmann, H., Burrows, J., Chevallier, F., Ciais, P., Crevoisier, C., Fix, A., Flamant, P., Frankenberg, C., Gibert, F., Heim, B., Heimann, M., Houweling, S., Hubberten, H., Jöckel, P., Law, K., Löw, A., Marshall, J., Agusti-Panareda, A., Payan, S., Prigent, C., Rairoux, P., Sachs, T., Scholze, M., and Wirth, M.: MERLIN: A French-German Space Lidar Mission Dedicated to Atmospheric Methane, Remote Sens., 9, 1052, https://doi.org/10.3390/rs9101052, 2017.

Frankenberg, C., Aben, I., Bergamaschi, P., Dlugokencky, E. J., Van Hees, R., Houweling, S., Van Der Meer, P., Snel, R., and Tol, P.: Global column-averaged methane mixing ratios from 2003 to 2009 as derived from SCIAMACHY: Trends and variability, J. Geophys. Res., 116, D04302, https://doi.org/10.1029/2010JD014849, 2011.

Giardino, C., Bresciani, M., Valentini, E., Gasperini, L., Bolpagni, R., and Brando, V. E.: Airborne hyperspectral data to assess suspended particulate matter and aquatic vegetation in a shallow and turbid lake, Remote Sens. Environ., 157, 48–57, https://doi.org/10.1016/j.rse.2014.04.034, 2015.

Guanter, L., Kaufmann, H., Segl, K., Foerster, S., Rogass, C., Chabrillat, S., Kuester, T., Hollstein, A., Rossner, G., Chlebek, C., Straif, C., Fischer, S., Schrader, S., Storch, T., Heiden, U., Mueller, A., Bachmann, M., Mühle, H., Müller, R., Habermeyer, M., Ohndorf, A., Hill, J., Buddenbaum, H., Hostert, P., Van Der Linden, S., Leitão, P., Rabe, A., Doerffer, R., Krasemann, H., Xi, H., Mauser, W., Hank, T., Locherer, M., Rast, M., Staenz, K., and Sang, B.: The EnMAP Spaceborne Imaging Spectroscopy Mission for Earth Observation, Remote Sens., 7, 8830–8857, https://doi.org/10.3390/rs70708830, 2015.

Guanter, L., Irakulis-Loitxate, I., Gorroño, J., Sánchez-García, E., Cusworth, D. H., Varon, D. J., Cogliati, S., and Colombo, R.: Mapping methane point emissions with the PRISMA spaceborne imaging spectrometer, Remote Sens. Environ., 265, 112671, https://doi.org/10.1016/j.rse.2021.112671, 2021.

Hancock, S. E., Jacob, D. J., Chen, Z., Nesser, H., Davitt, A., Varon, D. J., Sulprizio, M. P., Balasus, N., Estrada, L. A., Cazorla, M., Dawidowski, L., Diez, S., East, J. D., Penn, E., Randles, C. A., Worden, J., Aben, I., Parker, R. J., and Maasakkers, J. D.: Satellite quantification of methane emissions from South American countries: a high-resolution inversion of TROPOMI and GOSAT observations, Atmospheric Chem. Phys., 25, 797–817, https://doi.org/10.5194/acp-25-797-2025, 2025.

Hestir, E. L., Brando, V. E., Bresciani, M., Giardino, C., Matta, E., Villa, P., and Dekker, A. G.: Measuring freshwater aquatic ecosystems: The need for a hyperspectral global mapping satellite mission, Remote Sens. Environ., 167, 181–195, https://doi.org/10.1016/j.rse.2015.05.023, 2015.

Hu, H., Landgraf, J., Detmers, R., Borsdorff, T., Aan De Brugh, J., Aben, I., Butz, A., and Hasekamp, O.: Toward Global Mapping of Methane With TROPOMI: First Results and Intersatellite Comparison to GOSAT, Geophys. Res. Lett., 45, 3682–3689, https://doi.org/10.1002/2018GL077259, 2018.

Intergovernmental Panel On Climate Change (IPCC): Climate Change 2021 – The Physical Science Basis: Working Group I Contribution to the Sixth Assessment Report of the Intergovernmental Panel on Climate Change, 1st ed., Cambridge University Press, https://doi.org/10.1017/9781009157896, 2023.

https://doi.org/10.5194/egusphere-2026-3707
Preprint. Discussion started: 28 July 2026
© Author(s) 2026. CC BY 4.0 License.

Jacob, D. J., Turner, A. J., Maasakkers, J. D., Sheng, J., Sun, K., Liu, X., Chance, K., Aben, I., McKeever, J., and Frankenberg, C.: Satellite observations of atmospheric methane and their value for quantifying methane emissions, Atmospheric Chem. Phys., 16, 14371–14396, https://doi.org/10.5194/acp-16-14371-2016, 2016.

Jiang, Y., Zhang, L., Zhang, X., and Cao, X.: Methane Retrieval Algorithms Based on Satellite: A Review, Atmosphere, 15, 449, https://doi.org/10.3390/atmos15040449, 2024.

Jongaramrungruang, S., Frankenberg, C., Matheou, G., Thorpe, A. K., Thompson, D. R., Kuai, L., and Duren, R. M.: Towards accurate methane point-source quantification from high-resolution 2-D plume imagery, Atmospheric Meas. Tech., 12, 6667–6681, https://doi.org/10.5194/amt-12-6667-2019, 2019.

Kitchenham, B., Pearl Brereton, O., Budgen, D., Turner, M., Bailey, J., and Linkman, S.: Systematic literature reviews in software engineering – A systematic literature review, Inf. Softw. Technol., 51, 7–15, https://doi.org/10.1016/j.infsof.2008.09.009, 2009.

Lauvaux, T., Giron, C., Mazzolini, M., d'Aspremont, A., Duren, R., Cusworth, D., Shindell, D., and Ciais, P.: Global assessment of oil and gas methane ultra-emitters, Science, 375, 557–561, https://doi.org/10.1126/science.abj4351, 2022.

Leggesse, E. S., Zimale, F. A., Sultan, D., Enku, T., and Tilahun, S. A.: Corrigendum: Advancing non-optical water quality monitoring in Lake Tana, Ethiopia: insights from machine learning and remote sensing techniques, Front. Water, 6, 1489691, https://doi.org/10.3389/frwa.2024.1489691, 2024.

Lorente, A., Borsdorff, T., Butz, A., Hasekamp, O., Aan De Brugh, J., Schneider, A., Wu, L., Hase, F., Kivi, R., Wunch, D., Pollard, D. F., Shiomi, K., Deutscher, N. M., Velazco, V. A., Roehl, C. M., Wennberg, P. O., Warneke, T., and Landgraf, J.: Methane retrieved from TROPOMI: improvement of the data product and validation of the first 2 years of measurements, Atmospheric Meas. Tech., 14, 665–684, https://doi.org/10.5194/amt-14-665-2021, 2021.

Maasakkers, J. D., Varon, D. J., Elfarsdóttir, A., McKeever, J., Jervis, D., Mahapatra, G., Pandey, S., Lorente, A., Borsdorff, T., Foorthuis, L. R., Schuit, B. J., Tol, P., Van Kempen, T. A., Van Hees, R., and Aben, I.: Using satellites to uncover large methane emissions from landfills, Sci. Adv., 8, eabn9683, https://doi.org/10.1126/sciadv.abn9683, 2022.

Morozumi, T., Shingubara, R., Murase, J., Nagai, S., Kobayashi, H., Takano, S., Tei, S., Fan, R., Maximov, T. C., and Sugimoto, A.: Usability of water surface reflectance for the determination of riverine dissolved methane during extreme flooding in northeastern Siberia, Polar Sci., 21, 186–194, https://doi.org/10.1016/j.polar.2019.01.005, 2019.

Okoli, C. and Schabram, K.: A Guide to Conducting a Systematic Literature Review of Information Systems Research, SSRN Electron. J., https://doi.org/10.2139/ssrn.1954824, 2010.

Parker, R. J., Webb, A., Boesch, H., Somkuti, P., Barrio Guillo, R., Di Noia, A., Kalaitzi, N., Anand, J. S., Bergamaschi, P., Chevallier, F., Palmer, P. I., Feng, L., Deutscher, N. M., Feist, D. G., Griffith, D. W. T., Hase, F., Kivi, R., Morino, I., Notholt, J., Oh, Y.-S., Ohyama, H., Petri, C., Pollard, D. F., Roehl, C., Sha, M. K., Shiomi, K., Strong, K., Sussmann, R., Té, Y., Velazco, V. A., Warneke, T., Wennberg, P. O., and Wunch, D.: A decade of GOSAT Proxy satellite CH_4 observations, Earth Syst. Sci. Data, 12, 3383–3412, https://doi.org/10.5194/essd-12-3383-2020, 2020.

Sherwin, E. D., El Abbadi, S. H., Burdeau, P. M., Zhang, Z., Chen, Z., Rutherford, J. S., Chen, Y., and Brandt, A. R.: Single-blind test of nine methane-sensing satellite systems from three continents, Atmospheric Meas. Tech., 17, 765–782, https://doi.org/10.5194/amt-17-765-2024, 2024.

Suto, H., Kataoka, F., Kikuchi, N., Knuteson, R. O., Butz, A., Haun, M., Buijs, H., Shiomi, K., Imai, H., and Kuze, A.: Thermal and near-infrared sensor for carbon observation Fourier transform spectrometer-2 (TANSO-FTS-2) on the Greenhouse gases Observing SATellite-2 (GOSAT-2) during its first year in orbit, Atmospheric Meas. Tech., 14, 2013–2039, https://doi.org/10.5194/amt-14-2013-2021, 2021.

Tranvik, L. J., Downing, J. A., Cotner, J. B., Loiselle, S. A., Striegl, R. G., Ballatore, T. J., Dillon, P., Finlay, K., Fortino, K., Knoll, L. B., Kortelainen, P. L., Kutser, T., Larsen, S., Laurion, I., Leech, D. M., McCallister, S. L., McKnight, D. M., Melack, J. M., Overholt, E., Porter, J. A., Prairie, Y., Renwick, W. H., Roland, F., Sherman, B. S., Schindler, D. W., Sobek, S., Tremblay, A., Vanni, M. J., Verschoor, A. M., Von Wachenfeldt, E., and Weyhenmeyer, G. A.: Lakes and reservoirs as regulators of carbon cycling and climate, Limnol. Oceanogr., 54, 2298–2314, https://doi.org/10.4319/lo.2009.54.6_part_2.2298, 2009.

Tyler, A. N., Hunter, P. D., Spyrakos, E., Groom, S., Constantinescu, A. M., and Kitchen, J.: Developments in Earth observation for the assessment and monitoring of inland, transitional, coastal and shelf-sea waters, Sci. Total Environ., 572, 1307–1321, https://doi.org/10.1016/j.scitotenv.2016.01.020, 2016.

Varon, D. J., Jacob, D. J., McKeever, J., Jervis, D., Durak, B. O. A., Xia, Y., and Huang, Y.: Quantifying methane point sources from fine-scale satellite observations of atmospheric methane plumes, Atmos. Meas. Tech., 11, 5673–5686, https://doi.org/10.5194/amt-11-5673-2018, 2018.

Varon, D. J., Jervis, D., McKeever, J., Spence, I., Gains, D., and Jacob, D. J.: High-frequency monitoring of anomalous methane point sources with multispectral Sentinel-2 satellite observations, Atmospheric Meas. Tech., 14, 2771–2785, https://doi.org/10.5194/amt-14-2771-2021, 2021.

Veefkind, J. P., Aben, I., McMullan, K., Förster, H., De Vries, J., Otter, G., Claas, J., Eskes, H. J., De Haan, J. F., Kleipool, Q., Van Weele, M., Hasekamp, O., Hoogeveen, R., Landgraf, J., Snel, R., Tol, P., Ingmann, P., Voors, R., Kruizinga, B., Vink, R., Visser, H., and Levelt, P. F.: TROPOMI on the ESA Sentinel-5 Precursor: A GMES mission for global observations of the atmospheric composition for climate, air quality and ozone layer applications, Remote Sens. Environ., 120, 70–83, https://doi.org/10.1016/j.rse.2011.09.027, 2012.

Wachholz, A.: German small lake and pond inventory (GSLPI), https://doi.org/10.5281/ZENODO.14228168, 2024.

Wachholz, A., Schmidt, S. I., Arle, J., and Völker, J.: The German Small Lake and Pond Inventory, Earth Syst. Sci. Data, 18, 117–129, https://doi.org/10.5194/essd-18-117-2026, 2026.

Webb, J. R., Leavitt, P. R., Simpson, G. L., Baulch, H. M., Haig, H. A., Hodder, K. R., and Finlay, K.: Regulation of carbon dioxide and methane in small agricultural reservoirs: optimizing potential for greenhouse gas uptake, Biogeosciences, 16, 4211–4227, https://doi.org/10.5194/bg-16-4211-2019, 2019.

West, W. E., Coloso, J. J., and Jones, S. E.: Effects of algal and terrestrial carbon on methane production rates and methanogen community structure in a temperate lake sediment, Freshw. Biol., 57, 949–955, https://doi.org/10.1111/j.1365-2427.2012.02755.x, 2012.

West, W. E., Creamer, K. P., and Jones, S. E.: Productivity and depth regulate lake contributions to atmospheric methane, Limnol. Oceanogr., 61, https://doi.org/10.1002/lno.10247, 2016.